

## Single-channel activations and concentration jumps: comparison of recombinant NR1a/NR2A and NR1a/NR2D NMDA receptors

David J. A. Wyllie, Philippe Béhé and David Colquhoun

*Department of Pharmacology, University College London, Gower Street,  
London WC1E 6BT, UK*

(Received 2 February 1998; accepted after revision 17 March 1998)

1. We have expressed recombinant NR1a/NR2A and NR1a/NR2D *N*-methyl-D-aspartate (NMDA) receptor channels in *Xenopus* oocytes and made recordings of single-channel and macroscopic currents in outside-out membrane patches. For each receptor type we measured (a) the individual single-channel activations evoked by low glutamate concentrations in steady-state recordings, and (b) the macroscopic responses elicited by brief concentration jumps with high agonist concentrations, and we explore the relationship between these two sorts of observation.
2. Low concentration (5–100 nM) steady-state recordings of NR1a/NR2A and NR1a/NR2D single-channel activity generated shut-time distributions that were best fitted with a mixture of five and six exponential components, respectively. Individual activations of either receptor type were resolved as bursts of openings, which we refer to as ‘super-clusters’.
3. During a single activation, NR1a/NR2A receptors were open for 36% of the time, but NR1a/NR2D receptors were open for only 4% of the time. For both, distributions of super-cluster durations were best fitted with a mixture of six exponential components. Their overall mean durations were 35.8 and 1602 ms, respectively.
4. Steady-state super-clusters were aligned on their first openings and averaged. The average was well fitted by a sum of exponentials with time constants taken from fits to super-cluster length distributions. It is shown that this is what would be expected for a channel that shows simple Markovian behaviour.
5. The current through NR1a/NR2A channels following a concentration jump from zero to 1 mM glutamate for 1 ms was well fitted by three exponential components with time constants of 13 ms (rising phase), 70 ms and 350 ms (decaying phase). Similar concentration jumps on NR1a/NR2D channels were well fitted by two exponentials with means of 45 ms (rising phase) and 4408 ms (decaying phase) components. During prolonged exposure to glutamate, NR1a/NR2A channels desensitized with a time constant of 649 ms, while NR1a/NR2D channels exhibited no apparent desensitization.
6. We show that under certain conditions, the time constants for the macroscopic jump response should be the same as those for the distribution of super-cluster lengths, though the resolution of the latter is so much greater that it cannot be expected that all the components will be resolvable in a macroscopic current. Good agreement was found for jumps on NR1a/NR2D receptors, and for some jump experiments on NR1a/NR2A. However, the latter were rather variable and some were slower than predicted. Slow decays were associated with patches that had large currents.

It has been estimated that following the synaptic release of glutamate, the concentration in the synaptic cleft rises rapidly to around 1 mM and then decays with a time constant of about 1 ms (Clements, Lester, Tong, Jahr & Westbrook, 1992). Brief (1–5 ms) pulses of 1 mM glutamate to outside-out membrane patches containing *N*-methyl-D-

aspartate (NMDA) channels yield currents that decay over a few hundred milliseconds, which resemble the NMDA component of an excitatory postsynaptic current (EPSC) (Lester, Clements, Westbrook & Jahr, 1990; Edmonds & Colquhoun, 1992). Given the short duration of time that glutamate is available for binding to postsynaptic receptors

following release, and the slow rise and fall of currents through NMDA receptor channels, it is unlikely that an individual NMDA receptor would be activated more than once during a single synaptic event. The nature of these individual channel 'activations' is therefore considered to underlie the shape of the synaptic current (Lester *et al.* 1990; Gibb & Colquhoun, 1992; Lester & Jahr, 1992). The term 'activation' defines the sequence of events that takes place between the first opening that follows binding of agonist and the last opening before complete dissociation of agonist; the experimental estimate of this event is a 'super-cluster' (see Discussion for more rigorous definitions). The fact that two different molecules, a co-agonist and an agonist, are necessary to open the NMDA channel suggests that glycine as well as glutamate may determine the duration of NMDA single-channel activations. In all the experiments described here, however, glycine was used at a saturating concentration. Thus we expect the binding and unbinding of glutamate to the NMDA receptor complex (together with subsequent conformation changes) to determine the duration of receptor activations, as is presumably the case during synaptic transmission. Even under these conditions, however, the nature of such activations is complex, as illustrated by the equilibrium recordings of Gibb & Colquhoun (1991, 1992). They are far less well understood than, for instance, those of the nicotinic receptor at the neuromuscular junction (Colquhoun & Sakmann, 1985; Edmonds, Gibb & Colquhoun, 1995*a,b*), and no kinetic scheme is available that describes them adequately.

In this paper, we investigate the macroscopic response of NMDA receptors elicited by short (1 ms) pulses of glutamate and the structure of the super-clusters of channel activity elicited by very low glutamate concentrations, and explore the relationship between these two sorts of measurement. We have examined these issues for two recombinant NMDA receptors, namely NR1a/NR2A channels and NR1a/NR2D channels. In recordings from transfected human embryonic kidney (HEK) 293 cells, these two subunit combinations display the fastest and slowest offset rates, respectively, following the termination of a 300 ms application of 100  $\mu\text{M}$  glutamate (Monyer, Burnashev, Laurie, Sakmann & Seeburg, 1994), or following brief pulses of glutamate (Vicini *et al.* 1998).

We find that the macroscopic current decay following a 1 ms concentration jump on NR1a/NR2D channels decays much more slowly than that mediated by NR1a/NR2A receptors. We reach the same conclusion by comparing NR1a/NR2A and NR1a/NR2D super-cluster durations recorded in the steady-state experiments employing very low agonist concentrations.

A preliminary report of some of our findings has appeared previously (Wyllie, Béhé, Edmonds & Colquhoun, 1997).

## METHODS

Expression of NR1a/NR2A and NR1a/NR2D receptor channel cRNA for each of the NMDA receptor subunits was obtained as described previously (Béhé, Stern, Wyllie, Nassar, Schoepfer & Colquhoun, 1995; Wyllie, Béhé, Nassar, Schoepfer & Colquhoun, 1996). Oocytes were obtained from *Xenopus laevis* that had been anaesthetized by immersion in a 0.2% solution of tricaine (3-amino-benzoic acid ethyl ester), decapitated and pithed. Oocytes were defolliculated and injected with cRNA coding for NR1a and NR2A or NR1a and NR2D subunits (see Béhé *et al.* 1995 for details). The vitelline membrane of each oocyte was removed before making patch-clamp recordings. Oocytes were used 3–10 days after injection with cRNA.

### Steady-state recordings of single-channel activity

Low concentration (5–100 nM glutamate) recordings of recombinant NMDA channel activity in outside-out patches, held at  $-100$  mV, were made in an external solution containing (mM): 125 NaCl, 3 KCl, 1.25  $\text{NaH}_2\text{PO}_4$ , 20 Hepes and 0.85  $\text{CaCl}_2$ , plus 20  $\mu\text{M}$  glycine (pH 7.4 with NaOH). A free calcium concentration of 0.85 mM is equivalent to 1 mM total calcium in a bicarbonate buffer, as used in our earlier experiments on recombinant NMDA receptors. Patch-pipettes were made from thick-walled borosilicate glass (Clark Electromedical, Reading, UK) and filled with an 'internal' recording solution that contained (mM): 141 potassium gluconate, 2.5 NaCl, 10 Hepes and 11 EGTA (pH 7.4 with KOH). These solutions were chosen so that the reversal potential of  $\text{K}^+$  and  $\text{Cl}^-$  ions was  $-100$  mV. After fire-polishing of their tips, pipettes had resistances of 10–20 M $\Omega$ . Single-channel currents were recorded with an Axopatch-1D amplifier (Axon Instruments) and stored on digital audio tape (DAT) for subsequent analysis (Biologic DTR 1200/1205, Biologic Instruments, Claix, France).

### Concentration jump experiments

Fast concentration jumps on outside-out patches were achieved by the rapid switching, across the tip of the patch-pipette, of two solutions flowing from either side of a piece of theta-glass (type 14-072-01, Hilgenberg, Malsfeld, Germany). The internal and external recording solutions used for concentration jump experiments were the same as those used for steady-state single-channel recordings. The control solution was supplemented with 20  $\mu\text{M}$  glycine while the test solution contained 1 mM glutamate in addition to 20  $\mu\text{M}$  glycine. The theta-glass was moved by a piezo translator (model LSS-3200, Burleigh Instruments). Concentration jumps of 1 ms duration were made every 20 s in the case of NR1a/NR2A channels, or every 90 s for NR1a/NR2D channels, under computer control (CJUMP program; D. Colquhoun, University College London). Desensitization was examined by making long (4 s) applications of 1 mM glutamate. Measurement of liquid junction potentials indicated that the 20–80% rise-time for the exchange of control and test solutions was  $< 200$   $\mu\text{s}$ . Currents were recorded at a holding potential of  $-100$  mV (in one case  $-80$  mV), filtered at 2 kHz (NR1a/NR2A currents) or 200 Hz (NR1a/NR2D currents) and sampled at 10 kHz (or 1000 Hz) onto a computer hard disk via a CED 1401 plus interface (CED Instruments, Cambridge, UK). Individual sweeps were averaged and exponentials were fitted by the method of least-squares (CJFIT program; D. Colquhoun, University College London). When both rising and decaying phases were fitted, the total amplitude of all components was constrained to be zero.

### Analysis

Single-channel currents were replayed from DAT tape, filtered at 2 kHz and digitized continuously at 20 kHz. The amplitude and duration of events were fitted using the SCAN program (see Colquhoun & Sigworth, 1995). After fitting, the EKDIST program was used to impose consistent time resolution (usually 40–60  $\mu$ s for both openings and closings) on each data set, and to fit distributions by the method of maximum likelihood (Colquhoun & Sigworth, 1995). Distributions of all open periods were fitted with the mixture of three exponential components (the term ‘mixture’ is discussed in Colquhoun & Sigworth, 1995). Open periods are defined as a series of openings to one or more amplitude levels that contain no resolvable shuttings. For NR1a/NR2A receptors, shut-time distributions were fitted with a mixture of five exponential density functions. For NR1a/NR2D receptors, however, we found that the fitting of six components consistently gave better fits of the shut-time distributions than could be achieved with five components. In practice, ‘super-clusters’ of openings (Gibb & Colquhoun, 1992) were identified in the continuous data record as groups of openings that are separated from each other by a gap longer than a critical gap length ( $t_{\text{crit}}$ ). Values of  $t_{\text{crit}}$  were calculated between the fourth and the fifth component of NR1a/NR2A shut-time distributions, or between the fifth and the sixth component of NR1a/NR2D shut-time distributions. The gap duration chosen produced equal numbers of misclassified shut times, i.e. the number of events misclassified as being within a super-cluster when in fact they were between, was equal to the number misclassified as being between when in fact they were within a super-cluster (Magleby & Pallotta, 1983; Clapham & Neher, 1984; see Discussion). All shut times shorter than  $t_{\text{crit}}$  were defined as being *within* a super-cluster.

Distributions of super-cluster length and total open-time per super-cluster were constructed; they were each fitted with a mixture of exponential components. In addition, super-clusters were excised from the continuous record, inspected visually, aligned on their first opening and averaged; if the (fixed-length) sample being averaged contained any other openings after the end of the super-cluster, they were replaced by sections of baseline excised from other parts of the record. These averaged currents were then fitted with a sum of exponential components. All results are given as means  $\pm$  standard deviation of the mean, unless otherwise specified.

## RESULTS

### Low concentration steady-state single-channel recordings

Exposure of patches containing either NR1a/NR2A or NR1a/NR2D recombinant NMDA channels to a low concentration of glutamate in the continuous presence of a saturating concentration of glycine results in a low, steady-state single-channel activity, which in our experimental conditions can be recorded for several tens of minutes with no sign of run-down or run-up (see Stern, B  h  , Schoepfer & Colquhoun, 1992; Wyllie *et al.* 1996).

### Nature of activations

Figure 1 shows two 25 s stretches of steady-state channel activity (taken from recordings lasting 20 and 40 min, respectively) evoked by low concentrations of glutamate, in

**Figure 1. Steady-state activations of NR1a/NR2A and NR1a/NR2D channels activated by low concentrations of glutamate**

*A*, a continuous 25 s recording of NR1a/NR2A steady-state channel activity evoked by 100 nM glutamate (+ 20  $\mu$ M glycine). Activations of the channel are seen to occur in runs or trains of openings that we term ‘super-clusters’. *B*, a continuous 25 s recording of NR1a/NR2D channel activity evoked by 30 nM glutamate (+ 20  $\mu$ M glycine). It is clear that NR1a/NR2D super-clusters can last for several seconds, but the probability of the channel being open within an activation is lower than that seen for NR1a/NR2A activations. In each case, the horizontal bars above each series of openings indicates the time between the first opening and last closing of the activation.

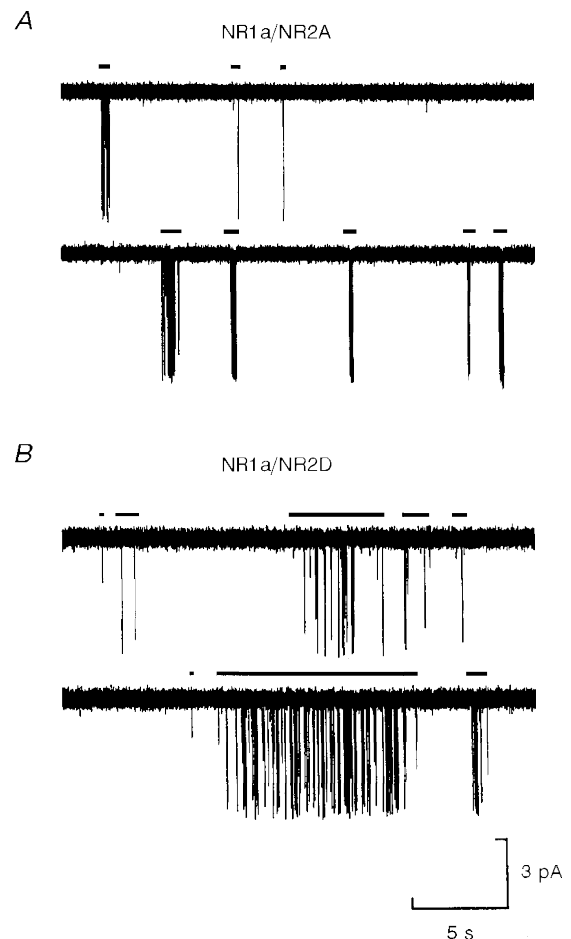


Table 1. Comparison of NR1a/NR2A and NR1a/NR2D shut times, open periods and super-clusters

		$\tau_1$ ( $\mu$ s)	$\tau_2$ (ms)	$\tau_3$ (ms)	$\tau_4$ (ms)	$\tau_5$ (ms)	$\tau_6$ (ms)	Distribution mean (ms)
NR1a/NR2A ( $n = 8$ )	Shut time	$45 \pm 8$ $40 \pm 3\%$	$0.498 \pm 0.08$ $22 \pm 2\%$	$4.86 \pm 0.78$ $17 \pm 2\%$	$28.9 \pm 4.6$ $8 \pm 1\%$	$7472 \pm 1750$ $13 \pm 3\%$	—	$1222 \pm 575$ —
	Open period	$62 \pm 4$ $31 \pm 2\%$	$1.01 \pm 0.13$ $16 \pm 2\%$	$3.64 \pm 0.51$ $54 \pm 3\%$	— —	— —	—	$2.12 \pm 0.26$ —
	Super-cluster length	$42 \pm 5$ $39 \pm 4\%$	$0.380 \pm 0.059$ $8 \pm 2\%$	$1.88 \pm 0.31$ $8 \pm 1\%$	$4.08 \pm 0.67$ $14 \pm 3\%$	$40.6 \pm 8.9$ $17 \pm 2\%$	$201 \pm 22$ $14 \pm 4\%$	$35.8 \pm 6.2$ —
	Open time per super-cluster	$63 \pm 10$ $41 \pm 3\%$	$1.60 \pm 0.32$ $22 \pm 3\%$	$14.7 \pm 3.5$ $30 \pm 2\%$	$150 \pm 29$ $7 \pm 2\%$	— —	— —	$12.5 \pm 1.5$ —
Super-cluster $P_{\text{open}} = 0.35 \pm 0.05$								
NR1a/NR2D ( $n = 4$ )	Shut time	$55 \pm 7$ $42 \pm 5\%$	$0.374 \pm 0.028$ $19 \pm 2\%$	$6.51 \pm 0.7$ $9 \pm 1\%$	$38.8 \pm 5.4$ $16 \pm 3\%$	$221 \pm 34$ $12 \pm 2\%$	$5061 \pm 343$ $2 \pm 0.5\%$	$128 \pm 36$ —
	Open period	$98 \pm 19$ $20 \pm 2\%$	$0.872 \pm 0.091$ $34 \pm 6\%$	$2.58 \pm 0.14$ $46 \pm 6\%$	— —	— —	—	$1.50 \pm 0.13$ —
	Super-cluster length	$71 \pm 16$ $8 \pm 4\%$	$1.03 \pm 0.44$ $18 \pm 5\%$	$4.71 \pm 0.89$ $14 \pm 3\%$	$65.6 \pm 15.5$ $6 \pm 2\%$	$1405 \pm 159$ $31 \pm 5\%$	$5174 \pm 1565$ $23 \pm 2\%$	$1602 \pm 196$ —
	Open time per super-cluster	$65 \pm 19$ $11 \pm 4\%$	$1.42 \pm 0.21$ $29 \pm 4\%$	$14.6 \pm 1.8$ $40 \pm 4\%$	$324 \pm 112$ $20 \pm 3\%$	— —	— —	$65.8 \pm 17.4$ —
Super-cluster $P_{\text{open}} = 0.04 \pm 0.02$								

Time constants for each component ( $\tau_1$  to  $\tau_6$ ) are given  $\pm$  s.d.m., together with their percentage areas.

the presence of 20  $\mu$ M glycine, mediated by NR1a/NR2A channels (Fig. 1A) or NR1a/NR2D channels (Fig. 1B). The horizontal bars above each trace indicate the beginning and end of separate trains of channel openings or super-clusters. Although Fig. 1 is shown on a time scale that makes it impossible to appreciate fine details of channel activation structure, two differences between activations of NR1a/NR2A and NR1a/NR2D channels are evident: NR1a/NR2D super-clusters are longer in duration than NR1a/NR2A ones, and the probability of the channel being open within an activation ( $P_{\text{open}}$ ) for NR1a/NR2D events is much lower (see Table 1).

### Open periods and shut times

Distributions of individual open periods, regardless of their amplitude, were best described by a mixture of three exponential components for both NR1a/NR2A and NR1a/NR2D channels. The mean values are given in Table 1. Both channel types have a subconductance level (Stern *et al.* 1992; Wyllie *et al.* 1996), and when distributions of open periods were constructed for the separate conductance levels, a total of four components were observed for each receptor subunit combination. Four components are not listed in Table 1, however, due to the fact that main and sub-

conductance open period distributions have some time constants in common. It is clear that the long-duration NR1a/NR2D super-clusters such as those illustrated in Fig. 1B do not result from the fact that the individual open periods of NR1a/NR2D channels are longer than those seen with NR1a/NR2A channels – they are in fact shorter, on average (see Table 1 and Stern *et al.* 1992; Wyllie *et al.* 1996).

Distributions of all shut times were constructed for each channel type. The shut-time distributions for the NR1a/NR2A receptor were fitted satisfactorily with five components while those of NR1a/NR2D channels required, consistently, six components. The mean values for each component are given in Table 1. It can be seen that the first four components are similar for both channel types, but that NR1a/NR2D shut time distributions require an extra component with a mean around 220 ms; this component is not detected in NR1a/NR2A distributions. Typical shut-time distributions from NR1a/NR2A and NR1a/NR2D channel recordings are illustrated in Fig. 2A and B.

In each shut-time distribution, a  $t_{\text{crit}}$  was identified as the gap most likely to separate individual super-clusters in the continuous record (see Methods). On average, values of  $t_{\text{crit}}$  were  $103 \pm 15$  ms for NR1a/NR2A channels and  $837 \pm$

100 ms for NR1a/NR2D channels. For NR1a/NR2A channels we observed clear separation between the fourth and fifth components of the shut-time distribution. Because of this the number of events that were misclassified as being within an activation when in fact they were between activations (and vice versa) was only  $1.9 \pm 0.3\%$  of the total number of events contained in these two components. There was poorer separation, however, of the last two components in NR1a/NR2D shut-time distributions. Although, on average, only  $3.8 \pm 0.7\%$  of the total number of events in the fifth and sixth components of NR1a/NR2D shut-time distribution were misclassified,  $15.4 \pm 1.9\%$  of events in the sixth component were actually considered to be *within* activations when they were in fact between activations. The implications of this are considered in the Discussion.

**Super-cluster length**

Histograms of super-cluster durations, identified on the basis of these  $t_{crit}$  values, were constructed. Super-clusters recorded in individual experiments were pooled and the resulting distributions for each channel type are shown in Fig. 3.

For both channel types, super-cluster distributions were fitted with a mixture of six exponential components. For NR1a/NR2A channels, the presence of at least four open states and four shut states within an activation implies that the super-cluster length distribution should contain eight components. By analogy, NR1a/NR2D super-cluster distributions should contain nine components. In either case, however, fitting super-cluster distributions with more than six components did not improve the quality of the fit.

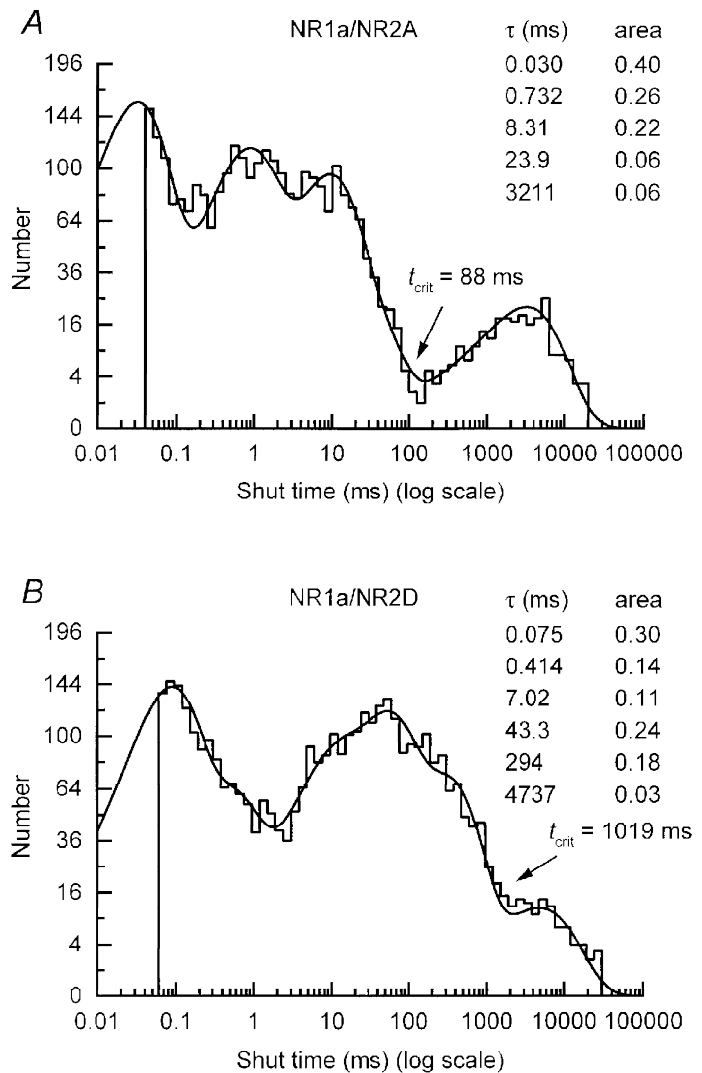
Distributions of total open time per burst were also obtained (not shown) and fitted with four components. The mean values for these fits are given in Table 1 for each receptor type.

Within a super-cluster, the probability of being open,  $P_{open}$ , can be defined as the ratio of the mean open time per super-cluster to the mean super-cluster length. For NR1a/NR2A channels the overall mean  $P_{open}$  within a super-cluster was  $0.36 \pm 0.05$ , while for NR1a/NR2D channels the  $P_{open}$  was much lower being, on average,  $0.04 \pm 0.02$ .

**Figure 2. Shut-time distributions for NR1a/NR2A and NR1a/NR2D channels**

*A*, shut-time distribution for glutamate-activated NR1a/NR2A channels (100 nM + 20  $\mu$ M glycine, same experiment as shown in Fig. 1*A*) fitted with a mixture of five exponentials with means (and areas) of 30  $\mu$ s (40%), 732  $\mu$ s (26%), 8.31 ms (22%), 23.9 ms (6%) and 3211 ms (6%). The fit predicts 4302 events and 2960 were included in the distribution, which has an overall mean of 183 ms.

*B*, shut-time distribution for NR1a/NR2D channels activated by glutamate (30 nM + 20  $\mu$ M glycine, same experiment as illustrated in Fig. 1*B*). The distribution is fitted with a mixture of six exponentials with means of 75  $\mu$ s (30%), 414  $\mu$ s (14%), 7.02 ms (11%), 43.3 ms (24%), 294 ms (18%) and 4737 ms (3%); 4568 events were predicted by the fit and 3734 events were included. The overall mean of the distribution is 225 ms.



### Alignment of super-clusters

Super-clusters identified in each recording were aligned on their first openings and averaged.

Figure 4A shows five individual NR1a/NR2A super-clusters, while Fig. 5A shows five NR1a/NR2D super-clusters. Comparison of these two figures shows first, that NR1a/NR2D super-clusters are much longer than those mediated by NR1a/NR2A receptors (note the difference in the time-base) and second, that the open probability within a super-cluster is quite different for each subtype. The longest NR1a/NR2D super-cluster we recorded was 45 s in duration, whereas NR1a/NR2A super-clusters never exceeded 1500 ms. We aligned (on their first opening) and averaged all super-clusters recorded throughout the course

of these experiments ( $n = 1403$  for NR1a/NR2A and  $n = 647$  for NR1a/NR2D) to verify that, for each combination, the decay generated from this procedure could be described by the same time constants that were identified by fitting the distribution of super-cluster durations. As explained in the Appendix, this must be the case for any Markovian mechanism. Figures 4B and 5B illustrate the average currents we obtained for NR1a/NR2A and NR1a/NR2D super-clusters, respectively. The white (dashed) curve superimposed on these current traces represents a sum of exponentials with the time constants fixed at the values found by fitting the respective super-cluster length distribution; the amplitude of each component was not constrained during the fitting procedure. Figure 4C shows an expanded time base illustration of the fit of the peak

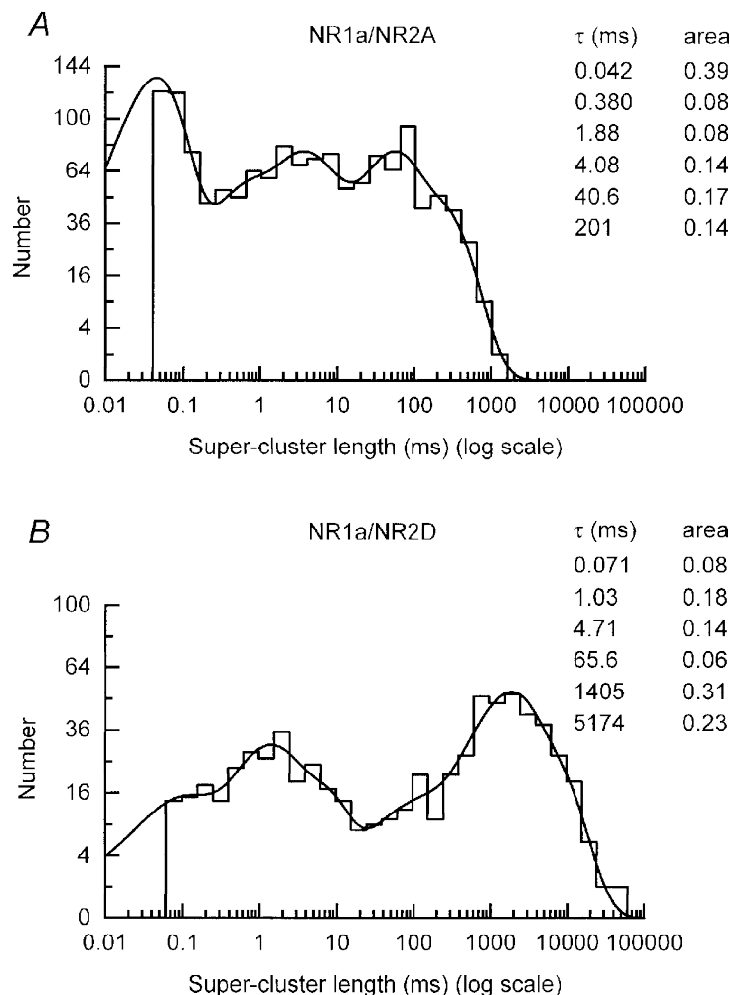


**Figure 3. Super-cluster distributions for NR1a/NR2A and NR1a/NR2D channels**

A, distribution of all NR1a/NR2A super-clusters (eight experiments were pooled). The distribution is fitted with a mixture of six exponentials with means of  $42 \mu\text{s}$  (39%),  $0.380 \text{ ms}$  (8%),  $1.88 \text{ ms}$  (8%),  $4.08 \text{ ms}$  (14%),  $40.6 \text{ ms}$  (17%) and  $201 \text{ ms}$  (14%). 1403 events were included in the fit while 1875 events were predicted. The overall mean of the distribution is  $35.8 \text{ ms}$ . B, distribution of all NR1a/NR2D super-clusters (four experiments were pooled). Again the distribution is fitted with six exponentials with means of  $71 \mu\text{s}$  (8%),  $1.03 \text{ ms}$  (18%),  $4.71 \text{ ms}$  (14%),  $65.6 \text{ ms}$  (6%),  $1405 \text{ ms}$  (31%) and  $5174 \text{ ms}$  (23%). 647 events were included in the fit and 689 events were predicted. The overall mean super-cluster length predicted by the fit is  $1602 \text{ ms}$ .

current of the NR1a/NR2A ‘aligned’ current. These fits again illustrate two main points. First, the NR1a/NR2D current decays considerably more slowly than the NR1a/NR2A current and second, the slowest components in each fit ( $\tau = 201$  ms and  $\tau = 5174$  ms for NR1a/NR2A and NR1a/NR2D, respectively) carry the vast majority of the charge.

**Concentration jumps on NR1a/NR2A and NR1a/NR2D channels**

Fast concentration jumps were performed on outside-out patches excised from oocytes in which either NR1a/NR2A receptors or NR1a/NR2D receptors were expressed.

Figure 6A shows two individual responses recorded following a 1 ms pulse of 1 mM glutamate, in an outside-out

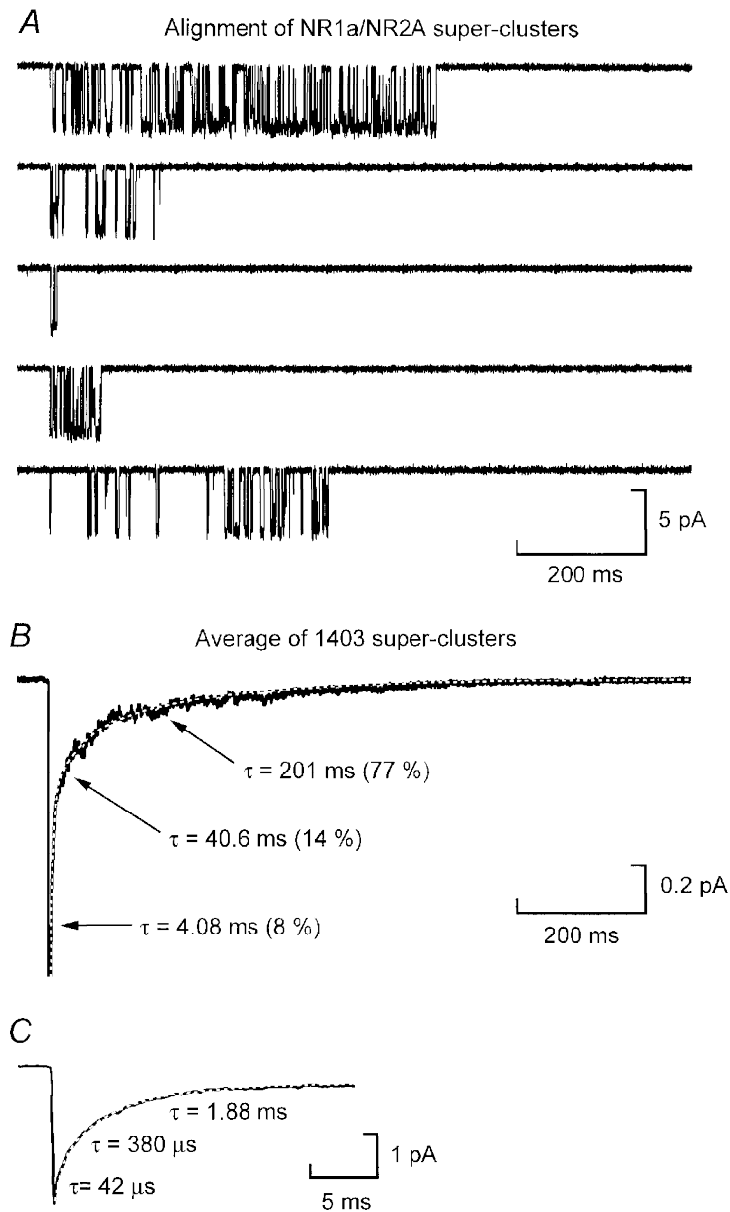


**Figure 4. Alignment of NR1a/NR2A super-clusters**

A, examples of five NR1a/NR2A super-clusters from the experiment illustrated in Figs 1A and 2A. The  $t_{crit}$  in this experiment was 88 ms. Note the example of a ‘high  $P_{open}$ ’ super-cluster (upper trace) and a super-cluster composed of only two apparent openings (middle trace). B, current obtained from the alignment and averaging of 1403 NR1a/NR2A super-clusters. The white dashed line shows the fit of these data with a sum of exponential components with time constants fixed at the values from the super-cluster distribution shown in Fig. 3A. The peak of this trace is truncated in this panel to allow clearer illustration of the slow decay of the current. C, expanded time-base illustration of the peak current to show the initial decay of the current fitted again with time constants obtained from the super-cluster length distribution fit shown in Fig. 3A. In B, the time constants are shown together with their respective relative areas.

patch that contained several channels. Single-channel currents are clearly visible in the traces, they have amplitudes of around 5 pA as expected for this 'high conductance' type of NMDA receptor at  $-100$  mV. The channel activity in the patch takes several hundred milliseconds to rise and decay, as is observed in a synaptic current mediated by NMDA receptors. The average of fifty such traces is shown in Fig. 6*B*. A pulse of agonist produces two relaxations, an 'on-relaxation' during the pulse and an

'off-relaxation', or 'deactivation', after the end of the pulse. In our case no current is detected during the 1 ms pulse, so essentially the whole of the observed signal, both rising and decaying phases, is an 'off-relaxation', the concentration of agonist being zero throughout. The current transient was fitted with the sum of three exponential components (one rising and two falling). Overall, the mean time constant for the rise-time was  $13.4 \pm 3.9$  ms, while the 'decay' was fitted with time constants with means of  $70.8 \pm 11.9$  and

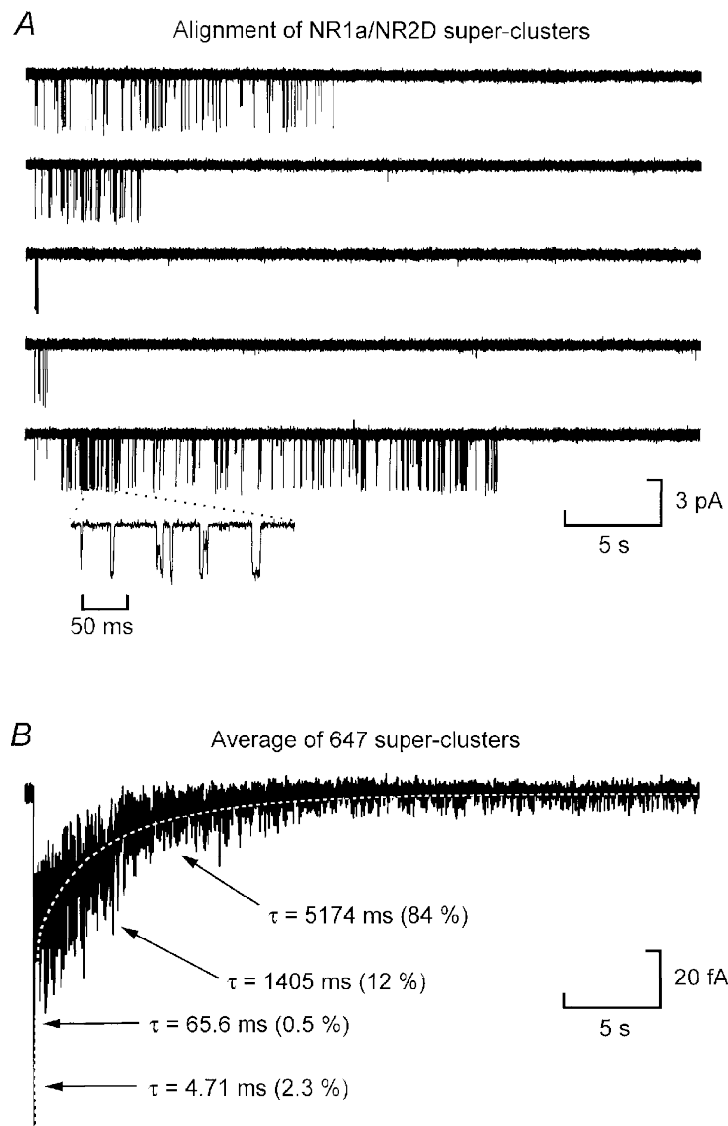


**Figure 5.** Alignment of NR1a/NR2D super-clusters

*A*, examples of NR1a/NR2D super-clusters from an experiment that gave a  $t_{\text{crit}}$  of 1019 ms (same experiment as Figs 1*B* and 2*B*). Like their NR1a/NR2A counterparts, NR1a/NR2D super-clusters can be comprised of only a few openings (third trace) but in contrast to NR1a/NR2A super-clusters, they can last for many seconds. Each of these traces show 35 s of activity. They also show periods of 'high  $P_{\text{open}}$ ' (bottom trace). The inset below the final super-cluster shows a 200 ms section of one of these 'high  $P_{\text{open}}$ ' periods on an expanded time-base. Overall, however, the  $P_{\text{open}}$  of NR1a/NR2D super-clusters is about 10-fold less than NR1a/NR2A super-clusters. *B*, average of 647 NR1a/NR2D super-clusters fitted with a sum of exponential components where the time constants have been fixed to those obtained from the fit of the distribution shown in Fig. 3*B*. The peak of this trace is truncated in this panel to allow clearer illustration of the slow decay of the current. This trace is digitally filtered at 50 Hz for illustration.



$350.1 \pm 39.4$  ms ( $n = 11$ ). The relative amplitudes of the two decaying components were  $59 \pm 8$  and  $41 \pm 8\%$ , respectively. However, the slowest component carries the majority of the charge, having a relative area of  $72 \pm 6\%$ .

During prolonged applications (4 s) of glutamate (1 mM), NR1a/NR2A receptor-mediated currents displayed marked desensitization (Fig. 6C and D); the NR1a/NR2A currents approached a steady-state level (on average  $28 \pm 8\%$  of the peak current value) with a time constant of  $649 \pm 57$  ms

( $n = 5$ ). This value is similar to the fast time constant reported for glutamate-induced desensitization of NR1a/NR2A channels expressed in HEK 293 cells (Medina *et al.* 1995).

The off-relaxation for the NR1a/NR2D receptor-channel was more than an order of magnitude slower than that for NR1a/NR2A.

Figure 7A shows the average of ten jumps recorded following a 1 ms pulse of glutamate. On average the rise and

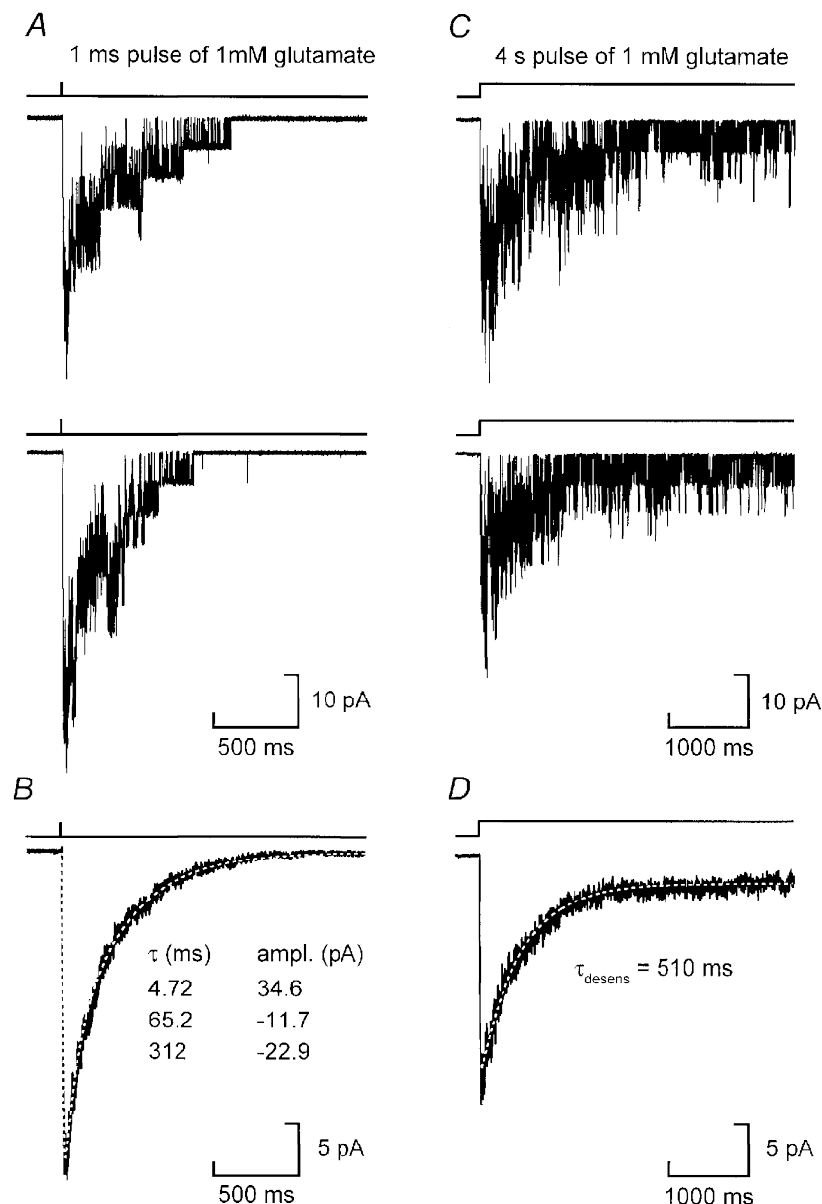


**Figure 6.** NR1a/NR2A macroscopic current responses to brief and prolonged exposure to agonist

*A*, two individual responses obtained from an outside-out patch following a 1 ms pulse of 1 mM glutamate (in the presence of  $20 \mu\text{M}$  glycine). Single-channel currents are clearly visible in these traces. *B*, the average of fifty such jumps fitted with the sum of three exponential components. *C*, two individual records obtained following a 4 s application of glutamate (1 mM). The channel activity declines during the prolonged application of agonist. *D*, average of sixty such sweeps. The decay of the current to a steady-state level is fitted with a single exponential with a time constant of 510 ms. All recordings were made at  $-100$  mV.

decay for the NR1a/NR2D channel appeared to be well described by only two exponential components with means of  $44.7 \pm 15.5$  and  $4408 \pm 354$  ms ( $n = 5$ ). Unlike NR1a/NR2A channels, NR1a/NR2D currents showed no detectable desensitization during prolonged exposure to agonist (Fig. 7*B*). For comparison the average traces for NR1a/NR2A and NR1a/NR2D ensemble currents are shown on the same time-base to illustrate the difference in off-relaxation kinetics for these two receptor combinations (Fig. 7*C*). The fact that following a brief concentration jump the NR1a/NR2D current decay on a time scale is similar to that seen for aligned NR1a/NR2D super-clusters, supports strongly our argument that single activations of NR1a/NR2D channels contain shut-times present in the first five components of NR1a/NR2D shut-time distributions.

### Relationship between concentration jumps and steady-state bursts

As shown in the Appendix, the time constants obtained from steady-state super-cluster length distributions and the time constants of the macroscopic response following a concentration jump should be the same or similar (see

Discussion for the precise conditions under which this is expected). We have tested this prediction for both NR1a/NR2A and NR1a/NR2D channels.

### NR1a/NR2D channels

The similarity of the responses following a 1 ms pulse of 1 mM glutamate in each of our experiments on NR1a/NR2D channels allowed us to pool data and to obtain an 'average' NR1a/NR2D macroscopic current (Fig. 8*A*). As mentioned above, the macroscopic response of NR1a/NR2D to a pulse of glutamate appeared, visually, to be satisfactorily described by only two exponential components, one for the rise (45 ms) and one for the decay (4408 ms) (see Fig. 7). However, the fit to the super-cluster length distribution suggests that six exponentials rather than two should be present. Two of these are too fast to be seen, but the remaining four should be observable. When the macroscopic current is fitted with four exponential components, with their time constants *fixed* at the values found by fitting the super-cluster length distribution and only their amplitudes allowed to vary, it is seen (Fig. 8*A*) that a good fit is obtained. In fact, in this case, a free fit of

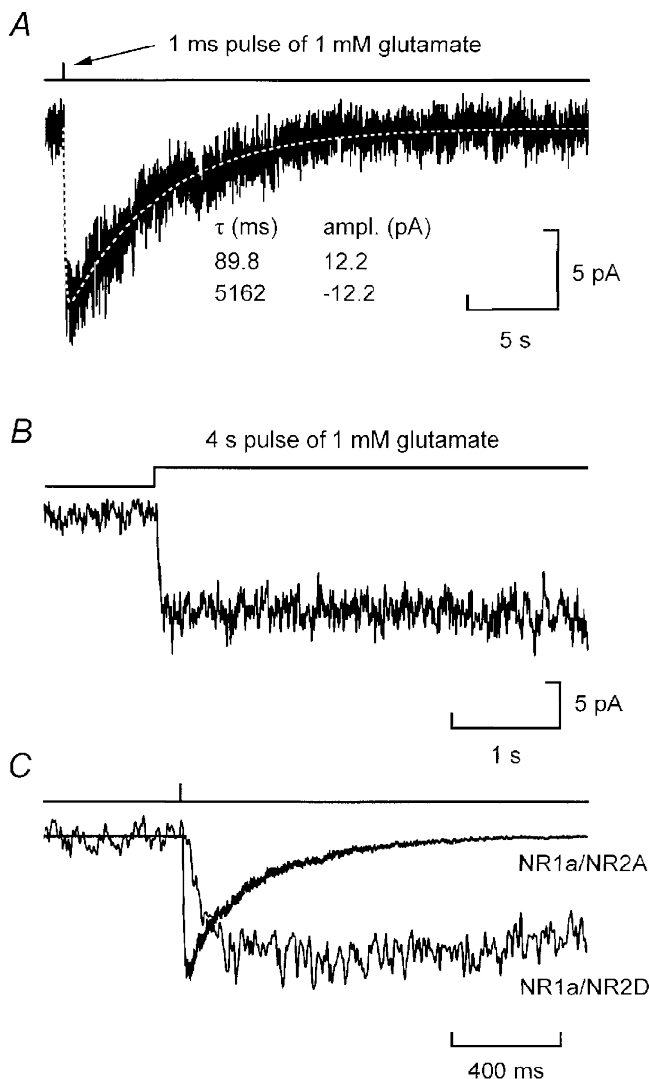


**Figure 7. NR1a/NR2D macroscopic current responses to brief and prolonged exposure to agonist**

*A*, average of ten jumps recorded from an outside-out patch containing NR1a/NR2D receptor channels following a 1 ms pulse of 1 mM glutamate (+ 20  $\mu$ M glycine). The off-relaxation of this current is well fitted with the sum of two exponentials, with time constants of 89.8 ms (rising) and 5162 ms (decay). *B*, average of ten sweeps illustrating that during prolonged agonist exposure, currents mediated by NR1a/NR2D channels are sustained, without visible desensitization. *C*, the same NR1a/NR2D-mediated current shown in *A*, but on an expanded time-base to illustrate the slower kinetics of this current when compared with NR1a/NR2A-mediated responses (same trace as shown in Fig. 6*B*). Currents have been scaled to have similar peaks. All recordings were made at  $-100$  mV.

four exponentials (using the super-cluster values as initial guesses) led to very similar time constants and amplitudes. Thus within the limitations of fitting exponentials to macroscopic currents, the predictions of the Appendix are verified.

**NR1a/NR2A channels**

In the case of NR1a/NR2A channels, however, there was considerably more variability in the macroscopic currents following a concentration jump than for NR1a/NR2D. This made it impossible to pool data from separate jump

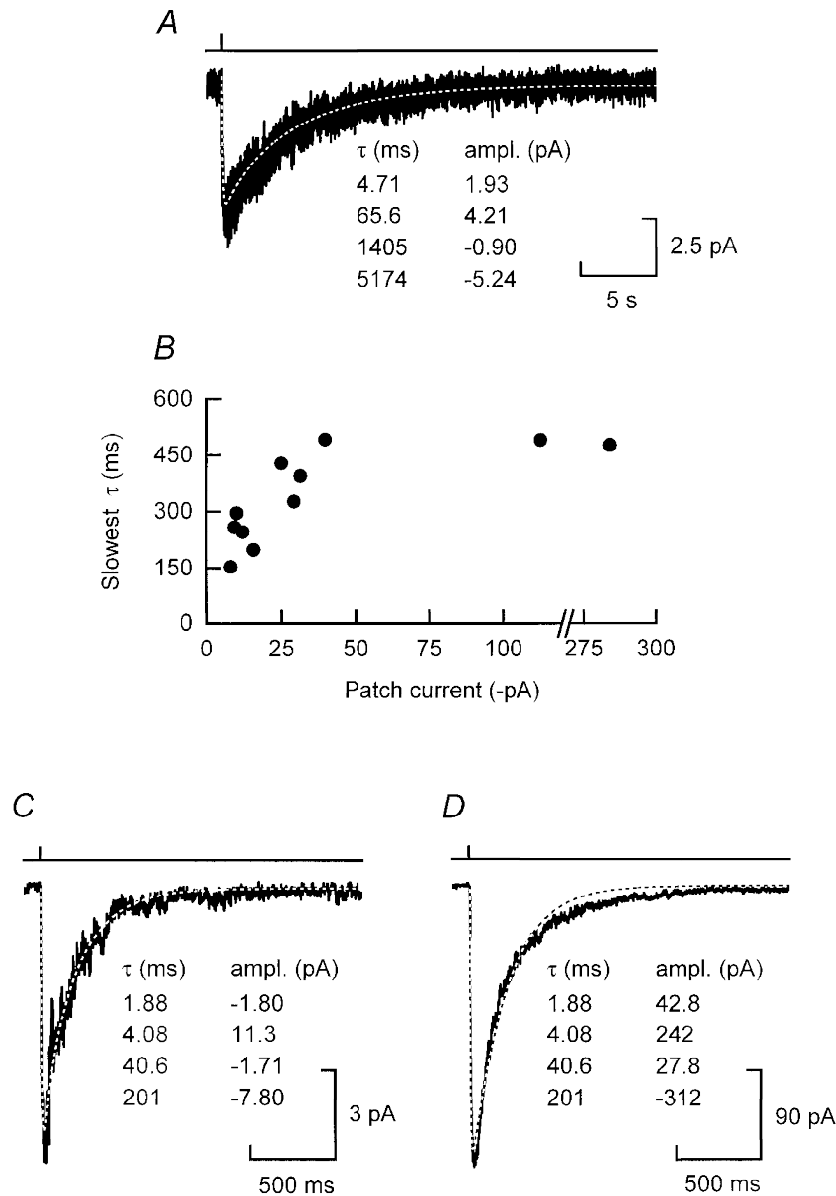


**Figure 8. NR1a/NR2A and NR1a/NR2D macroscopic jumps fitted with time constants obtained from super-cluster distributions**

A, 'average' NR1a/NR2D macroscopic current obtained following a 1 ms pulse of 1 mM glutamate. Data from five individual jump experiments on NR1a/NR2D receptor channels were pooled and averaged. The dashed white line shows the best least-squares fit of these data by a sum of four exponentials where the time constants were *fixed* at the values obtained from the super-cluster distribution shown in Fig. 3B. B, plot of the magnitude of the peak current *versus* the value of the slowest decay time constant for macroscopic jump experiments on outside-out patches containing NR1a/NR2A channels. It appears that patches giving the smallest currents possess the fastest decay time constants. C, an example of a macroscopic current (peak current, ~10 pA) recorded following a 1 ms pulse of 1 mM glutamate, which was well fitted by a sum of four exponentials with time constants *fixed* to the values obtained from the fit of NR1a/NR2A super-cluster lengths (Fig. 3A). D, an example of a macroscopic current that had a large peak current (~300 pA) and is fitted poorly by the sum of four exponentials with the same set of time constants as used in C.

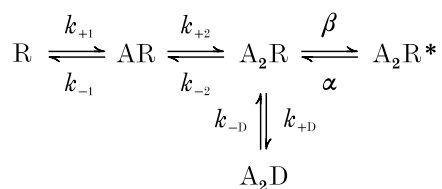
experiments. Indeed we noted a correlation between the magnitude of the macroscopic current and the value of the slowest time constant (Fig. 8*B*). Possible reasons for this correlation are mentioned in the Discussion. Figure 8*C* and *D* shows responses obtained in two different experiments taken from the extremes of our data set. The current illustrated in Fig. 8*C* is quite well described by the time constants taken from the NR1a/NR2A super-cluster distribution (Fig. 3*A*) whereas the current shown in Fig. 8*D* decays considerably more slowly than expected. The fit shown is the best least-squares fit of the data with the fixed time constants. The range of values for the slower decay time constant for the jump experiments was 153 ms to 517 ms ( $n = 11$ ). However, none of the individual super-cluster length distributions had a time constant as slow as the slowest jumps, the range for the slowest time constant for the former being 133 ms to 287 ms ( $n = 8$ ). In the Discussion we will address to what extent our data for NR1a/NR2A channels agree with the predictions of the Appendix.

## DISCUSSION

Before discussing the interpretation of our results, it is essential to define with greater precision than before, the meaning of some of the terms that we use. After that we shall consider the extent to which the results comply with the predictions in the Appendix, and possible reasons for discrepancies, before going on to the general features of the results and their relation to other work.

### Some basic definitions

For simplicity, we will illustrate the general definitions by reference to the kinetic model proposed by Lester & Jahr (1992). Even though this model is too simple to account for observations made in single-channel recordings (i.e. the presence of multiple conductance levels, multiple open and closed states and correlations of open and shut times), it will be useful to clarify our discussion. It is shown as Scheme 1:



Scheme 1

In this scheme two agonist molecules (A) bind to the receptor (R), which may then either open ( $A_2R^*$ ), or enter a rather long-lived shut state ( $A_2D$ ).

It is important at this stage to be clear about the definitions of the terms burst, super-cluster and activation.

### Definition of an activation

By the term ‘activation’ we mean the unitary set of one or more openings that are produced by agonist binding. The

crucial property that defines activations is that they must become progressively further and further apart as the agonist concentration is reduced. In general, this definition implies that partially liganded shut states may form part of an activation. Thus in general, an activation is ended by a shut interval that contains one or more sojourns in the vacant state (e.g. R in Scheme 1).

The term ‘super-cluster’ is used here for consistency with Gibb & Colquhoun (1992), who defined several sorts of bursts in steady-state records, the longest of which they termed a super-cluster, and they suggested that this type of burst corresponded to a single activation of the channel. In this Discussion we shall consider only this sort of burst. A burst is itself defined in two different ways, which may be termed the mechanistic definition and the experimental definition. The former is defined in terms of some postulated mechanism (and, when appropriate states are included in the burst, it means the same thing as ‘activation’), whereas the latter is defined empirically in terms of a specified  $t_{\text{crit}}$  (see Methods). The latter is an experimental estimate of the former, and insofar as it is an accurate estimate, it allows empirical observations of bursts to be interpreted in terms of underlying mechanisms.

### The mechanistic definition of bursts

In general, a burst is defined by dividing the states in which the receptor can exist into three subsets, A, B and C (Colquhoun & Hawkes, 1982). Set A contains the open states, set B contains short-lived shut states and set C contains long-lived shut states. The shut times *within* a burst are spent entirely within B states, and the shut times between bursts are spent in any sequence of shut states, which includes at least one sojourn in a long-lived C state. Thus a burst is spent entirely within sets A and B which, jointly, are the ‘burst states’, denoted set E. Whether or not such bursts can be distinguished in practice depends on the agonist concentration, the mechanism, and the particular values of the rate constants in it. For example, although the individual states in set B may all be short-lived, if there are many oscillations between these states then the total length of the sojourn in set B, the within-burst shut time, may not itself be short. Hence it is necessary to define B states such that total length of the sojourn within them is almost always shorter than the length of any shut time that includes a sojourn in a state in set C. If this can be done successfully, then the distribution of all shut times will have well-separated components that correspond to shut sojourns that do not enter a C state (within bursts) and those that do (between bursts). In this case it will be possible to use the shut-time distribution to define a  $t_{\text{crit}}$  that allows bursts to be defined from an experimental record that correspond closely to the mechanistic definition.

Which sojourns are short and which are long will, of course, depend on the agonist concentration. For example, the monoliganded state (AR) in Scheme 1 has a mean lifetime that increases as the agonist concentration is reduced,

tending towards  $1/k_{-1}$  as the concentration approaches zero. However, it is not only the mean lifetime of AR that matters, but also the fact that when the agonist concentration is very low, a channel that reaches AR is very likely to move next to the long-lived vacant state (R), rather than to re-bind an agonist molecule with the consequent possibility of re-opening. For example, with the rate constants used for Scheme 1 by Lester & Jahr, and an agonist concentration of 30 nM, a channel in state AR has a 97% chance of dissociation and a 3% chance of re-association. Thus re-openings after reaching AR will be very rare, and state AR should be part of set C, not set B (this is essential at zero concentration, as explained in the Appendix). At higher agonist concentrations there will, of course, be more re-openings after reaching AR, and the passage from the open state to AR and back to open will usually take longer than passage to  $A_2R$  and back, so a longer class of shut times will be created. Unless the former are sufficiently longer than the latter for the two types to be discriminated clearly from each other, it would become necessary, at higher agonist concentrations, to redefine the subsets so that state AR was also in set B ('within burst shut states'). A small intermediate length class of shut times within bursts is indeed seen with the muscle nicotinic receptor, and it may result from return to the doubly liganded open state after reaching the singly liganded shut state (Colquhoun & Sakmann, 1985).

When the agonist concentration is zero, following a concentration jump, it becomes essential (see Appendix) to include in set C all states from which re-opening becomes impossible at zero agonist concentration. Thus in Scheme 1, an activation is spent in state  $A_2R^*$  (open), or in shut states  $A_2R$  or  $A_2D$ , from which the open state may be reached even at zero agonist concentration (these are denoted sets A and B, respectively, in the Appendix, set C consisting of states R and AR from which the channel can never open at zero concentration). Thus all shut times within a super-cluster must be spent in states  $A_2R$  or  $A_2D$ .

### The experimental definition of bursts: distinguishing super-clusters in experimental records

As described in the Methods section, super-clusters of channel openings were obtained by recording from low channel density patches using very low agonist concentrations in an attempt to achieve clear separation of individual activations. The longest component in the shut time distribution was considered to represent shut times that are *between* super-clusters. In practice there are several problems. The exponential components overlap, so no value of  $t_{\text{crit}}$  can achieve perfect separation between them. Three ways of defining  $t_{\text{crit}}$  are in common use (e.g. Colquhoun & Sigworth, 1995), and many more are reasonable, but there is no way to choose which value is optimum in the absence of detailed knowledge of the mechanism. This is not surprising because the exponential components, on which the usual methods for finding  $t_{\text{crit}}$  are based, are themselves, in

general, a mathematical abstraction, and do not correspond precisely to any particular physical events, though in some cases they may be close to doing so.

For NR1a/NR2A shut-time distributions, the fourth and fifth components showed clear separation, which resulted in only  $1.9 \pm 0.3\%$  of events being misclassified. We therefore expect no appreciable error in either the identification of the gaps that separate activations, nor consequently in our estimate of the NR1a/NR2A super-cluster length. The situation is, however, less favourable in the case of the NR1a/NR2D channels. There is a substantial overlap of the fifth and sixth components in their shut-time distributions. On average, 15% of shut times in the sixth component of the shut-time distribution were below  $t_{\text{crit}}$ , and so were misclassified as being within, rather than between, bursts.

### Is the prediction of the Appendix verified?

The Appendix establishes an important relationship between the two sorts of observations that were obtained during our patch-clamp experiments. It shows that super-cluster length distributions (and the time course of super-clusters averaged after alignment) obtained from steady-state low concentration experiments should have the same number of exponential components, with the same values for their time constants, as the relaxation following a 1 ms pulse of 1 mM glutamate in concentration jump experiments.

However, this conclusion will be true only if (a) the process of extracting super-clusters from a steady-state record is adequate, and (b) the transitions rates between the 'burst states' (set E), and for leaving these states, are independent of concentration over the relevant range (e.g. 30 nM for steady-state recordings rather than the zero concentration that obtains for almost all of the macroscopic jump). In other words  $Q_{\text{EE}}$  (Appendix, eqn (A3)), and hence the time constants, must be independent of concentration. This will be true if all these states are fully liganded (e.g. states  $A_2R^*$ ,  $A_2R$  and  $A_2D$  in the case of Scheme 1). If the burst is defined to contain partially liganded shut states (see below, e.g. AR in Scheme 1) and/or partially liganded open states, it will be, at best, an approximation. In this case the initial condition at the moment the concentration is stepped to zero (defined by  $p_{\text{E}}(0)$  in Appendix, eqn (A3)), and the initial condition at the start of a steady-state burst ( $\phi_{\text{b}}$  in Appendix eqns (A1) and (A5)), may depend strongly on concentration. This will alter the relative *amplitudes* of the components (and hence the appearance and overall mean), but it will *not* affect the time constants that depend only on  $Q_{\text{EE}}$ .

In the case of NR1a/NR2D receptors, our results agree very well with the prediction. The results also underline the vastly superior resolution of single-channel measurements in comparison with measurements of macroscopic currents (see Results). For NR1a/NR2A channels, however, the time course measured in different experiments was rather variable, and only the fastest jumps showed good agreement

with the prediction (see Fig. 8). The possible sources of error will next be discussed by considering points (a) and (b), mentioned above.

**(a) Is the process of extracting super-clusters from a steady-state record adequate?**

All the results shown were found using a value of  $t_{\text{crit}}$  that produced equal numbers of misclassified short and long shut times (criterion of Magleby & Pallotta, 1983, and Clapham & Neher, 1984). Compared with this, the value of  $t_{\text{crit}}$  that minimized the *proportions* of misclassified events (Colquhoun & Sakmann, 1985) was (when defined) smaller, and the value that minimized the *total* number of misclassifications (Jackson, Wong, Morris, Lecar & Christian, 1983) was larger.

For NR1a/NR2A, the clear separation of the fourth and fifth components of shut-time distributions meant that the estimates of super-cluster length were insensitive to the value of  $t_{\text{crit}}$ , as discussed above.

Despite the good agreement with predictions found for the NR1a/NR2D receptor, it should be noted that the separation of the last component of their shut-time distributions was less clear (see above). If the criterion of Jackson *et al.* (1983) was used to define NR1a/NR2D super-clusters, a substantially longer slow component was seen in the distribution of super-cluster lengths, so this uncertainty about the best  $t_{\text{crit}}$  value, together with the relatively small number of super-clusters, limits the precision of our conclusions about NR1a/NR2D channels.

**(b) Are the time constants for activations dependent on concentration?**

The simplest form of concentration dependence would arise if the concentration used for the steady-state experiments were sufficiently high to result in a significant number of re-openings of the channel after it had returned to a partially liganded state (e.g. AR in Scheme 1). This seems rather unlikely at the very low concentrations that were used in our experiments, as mentioned above. A more serious possibility is that partially liganded receptors might themselves be able to open. This cannot happen in Scheme 1, but it is thought to happen for the muscle nicotinic receptor (e.g. Colquhoun & Sakmann, 1985; Jackson, 1988). Whether events such as these, which result in  $Q_{\text{EE}}$  being concentration dependent, occur with NMDA receptor channels remains to be determined, but if they do, then the time constants for receptor activations may depend significantly on agonist concentration. Preliminary data obtained by performing high concentration jumps on a patch containing a single NR1a/NR2A NMDA channel, suggest that similar open and shut states are accessed under these conditions as are accessed in low concentration experiments (see Wyllie, Edmonds & Colquhoun, 1997). The fact that we observe a good agreement with prediction for NR1a/NR2D, and at least the faster NR1a/NR2A jumps, suggests that concentration dependence of this sort is not playing a major role under our conditions, and the reasons

for some NR1a/NR2A jumps being slower than expected is likely to come from some other source.

Activations may exhibit a different sort of concentration dependence if the channels are modulated to an extent that depends on the magnitude of the agonist-evoked current. The amount of current flowing through the outside-out membrane patch is certainly very different in our two experimental conditions. If such a phenomenon were to cause discrepancies between the decays of aligned super-clusters and of macroscopic jumps, then we might expect those patches that gave the highest peak current in our jump experiments to have slower decays. It is therefore interesting to note that we observe such a correlation (Fig. 8B). This correlation is in the opposite direction from that which might be expected if there were variable amounts of contaminant zinc (Paoletti, Ascher & Neyton, 1997). Whether an elaborate second messenger system that alters channel kinetics is at work, and what role the incoming ions play, has not been investigated. On the basis of the Lester & Jahr model, the only way to prolong the time constant of the long component of the post-jump relaxation while decreasing the  $P_{\text{open}}$  is to increase the rate of entry into the long-lived closed state and/or the time spent in it.

In summary, the fact that the same time constants are found for the super-cluster length distribution and for the time course of aligned averaged super-clusters is exactly what is expected for an ion channel that behaves in a simple Markovian manner. Other sorts of mechanism have been advocated, for example semi-Markov (Ball, Yeo, Milne, Edeson, Madsen & Sansom, 1993), or fractal or chaotic kinetics (see Liebovitch & Todorov, 1996). Clearly there is no need to invoke such mechanisms to explain our results. To the extent that macroscopic jumps are also described by the same time constants, they too confirm this conclusion.

**General features of NR1a/NR2A and NR1a/NR2D channel activity**

NR1a/NR2D currents evoked by a 1 ms concentration jump decayed by an order of magnitude more slowly than those mediated by NR1a/NR2A channels. Assuming that the channel can be active only when the agonist is bound, it appears that glutamate remains on NR1a/NR2D channels for considerably longer than it does on NR1a/NR2A channels.

The long duration of NR1a/NR2D activations does not arise from the fact that individual open periods are longer for NR1a/NR2D channels than they are for NR1a/NR2A channels (in fact they are shorter), but rather from the presence of many long shut times ( $\tau = 221$  ms) within these activations. We could find no evidence for a similar slow component in NR1a/NR2A shut-time distributions, which required one fewer components than the shut-time distributions for NR1a/NR2D. Therefore we have to conclude that either the NR1a/NR2D channel has an additional long-lived shut state not present in NR1a/NR2A, or that the corresponding state for the NR1a/NR2A

channel is either too rarely visited, or gives rise to a component with a time constant too similar to that of another component, so that it cannot be detected.

The presence of these long-lasting shut states in NR1a/NR2D activations results in a very low probability of a NR1a/NR2D channel being open during an activation – they are closed, on average, for 96% of the super-cluster duration. Despite this fact, when differences in mean super-cluster length,  $P_{\text{open}}$  and single-channel conductance for NR1a/NR2A and NR1a/NR2D channels are taken into account, single activations of NR1a/NR2D receptors still carry roughly three times more charge than their NR1a/NR2A counterparts.

The slow rise of synaptic NMDA receptor-mediated currents is likely to arise from the fact that the channel can enter several long-lived shut states, following agonist binding but before opening. Indeed, following a 1 ms jump of 1 mM glutamate onto a patch containing one NR1a/NR2A channel, we have been able to measure directly these so-called first latencies. Our preliminary data give a mean value of between 20 and 30 ms for this parameter (Wyllie *et al.* 1997), which is similar to the value suggested by MK-801 block of NMDA-mediated currents in rat cultured hippocampal neurones (Dzubay & Jahr, 1996). However, direct comparison is limited due to the uncertainty of the NMDA receptor subunit composition in these neurones. As pointed out in the Appendix, channels that have a long first latency must necessarily give rise to some long activations.

### Comparison with other work

The concept of aligning super-clusters as a means of obtaining information about the nature of the decay of synaptic currents was originally described by Edmonds & Colquhoun in 1992. In their study of NMDA receptors in dentate granule cells, they found that the decay of aligned super-clusters and super-cluster length distributions did not appear to share the same set of time constants. Their suggestion that this discrepancy could be explained in part by the existence of a long first latency was, as shown in the Appendix, incorrect. In their study, the aligned super-cluster decay did not appear to contain the slow ( $\approx 300$  ms) component present in super-cluster length distributions. The small amplitude of this component in the aligned super-cluster decay most probably prevented its detection. The shut-time distributions analysed in the study of Edmonds & Colquhoun gave a value for the fourth shut-time component of 360 ms, considerably longer than our value of 29 ms (perhaps because the native receptor was not NR1a/NR2A). This resulted in a value of the  $t_{\text{crit}}$  used to define super-clusters of 642 ms (compared with our value of 103 ms). A longer  $t_{\text{crit}}$  will obviously lead to longer duration super-clusters which will, however, have a lower  $P_{\text{open}}$ . This would make the fitting of aligned activations more difficult because the amplitude of the slow component would be small. It should be noted, however, that the shut-time distribution

illustrated in Fig. 2A of Edmonds & Colquhoun (1992) can be fitted equally well (statistically indistinguishably) by placing the fourth component at around 30 ms (instead of 314 ms as illustrated), thus agreeing with the mean value we report for  $\tau_4$  in NR1a/NR2A shut-time distributions in our present study.

The time constants we obtained for NR1a/NR2A decay are slower than those reported by Vicini *et al.* (1998). In their study in which they expressed NR1a and NR2A subunits in HEK 293 cells, they obtained decay time constants of 33 and 247 ms. In addition, there appear to be differences in the relative amplitudes of the two time constants describing the decay of the current in HEK 293 cells compared with our data from oocytes; in HEK 293 cells the relative amplitude of the faster component is  $90 \pm 8\%$ . The reasons for these differences are unclear, but may result from the different expressions systems, and/or recording solutions, used in the two studies.

### Physiological implications

The NR2A NMDA receptor subunit is widely distributed throughout the CNS and receptors that contain it are thought to mediate EPSCs at many central synapses. As yet, however, there is no clear evidence that the NR1a/NR2D receptor channels mediate synaptic currents. The slow kinetics of the NR1a/NR2D channels would mean that any synaptic current mediated by this subunit combination would last several seconds – a duration of action normally associated with second messenger-linked receptors.

Cerebellar Purkinje neurones are known to contain mRNA for the NR2D receptor subunit (Akazawa, Shigemoto, Bessho, Nakanishi & Mizuno, 1994) and possess NMDA receptors with single-channel conductances identical to those of recombinant NR1a/NR2D channels (Momiya, Feldmeyer & Cull-Candy, 1996; Wyllie *et al.* 1996). Despite expressing somatic NR1a/NR2D-like channels during the first postnatal week of development, Purkinje cells lack any NMDA-mediated synaptic current (Momiya *et al.* 1996). In the spinal cord, however, slowly rising and falling EPSCs lasting up to 15 s can be evoked in dorsal horn neurones following 1–10 Hz stimulation of primary afferents (Miller & Woolf, 1996). These currents are attenuated by the NMDA receptor antagonist, D-2-amino-5-phosphopentanoic acid. Dorsal horn neurones also express NR2D mRNA transcripts (Monyer *et al.* 1994) and contain NMDA receptor channels likely to contain NR2D receptor subunits (Momiya *et al.* 1996). It is therefore tempting to speculate that these slow EPSCs were mediated by NR2D-containing NMDA receptors. It is not yet certain whether NR2D-containing NMDA receptors can be activated synaptically, or whether they are extrasynaptic.

It is also quite likely that NR2D-containing receptors would be activated tonically by ambient glutamate, because their response is sustained, and they have relatively low sensitivity to voltage-dependent  $\text{Mg}^{2+}$  block (Kuner &

Schoepfer, 1996; Wyllie *et al.* 1996). This would result in a slow but long-lasting  $\text{Ca}^{2+}$  entry into any cell expressing this particular receptor. Such processes are likely to be important in Hebbian synapse formation where pre- and postsynaptic activity need to be co-ordinated – the slow kinetics of NR1a/NR2D receptors would allow for a certain degree of temporal flexibility in such a system. In this respect it is interesting to note that the expression of NR2D appears to peak in early development (Monyer *et al.* 1994).

## APPENDIX

### The time course of jumps, averaged aligned bursts, and the distribution of burst length

General expressions for the time course of jumps were given by Colquhoun & Hawkes (1977), and for distributions of the burst length by Colquhoun & Hawkes (1982). Single channels after a jump are analysed by Colquhoun, Hawkes, Merlushkin & Edmonds (1997). An introduction to the notation and results is given by Colquhoun & Hawkes (1995*a,b*). We give these results here, and compare them with the expected time course for aligned bursts. The general term *burst* is used in this Appendix; the bursts of interest in the paper are the channel activations, which are estimated as super-clusters.

#### Notation

The kinetic mechanism is defined by a matrix,  $\mathbf{Q}$ , which has the transition rates between states as its off-diagonal elements, and diagonal elements defined to make its rows sum to zero. The time constants for observable events depend only on the value of  $\mathbf{Q}$  at the time of the measurement, but the amplitudes or areas depend also on the initial condition or ‘entry probabilities’, the state of the system at the start of the event. For example, we shall be interested in the fraction of channels that are in each state at zero time (at the moment the concentration is stepped to zero, i.e. at the end of the concentration pulse, in our case), and these are specified in a  $(1 \times k)$  row vector  $\mathbf{p}(0)$ . In the case of bursts measured in the steady state we similarly need to know the relative probability of being in each of the *open* states at the moment a burst starts; this can be calculated as shown by Colquhoun & Hawkes (1982), and is the  $(1 \times k_A)$  row vector  $\boldsymbol{\phi}_b$  defined there.

For the purposes of analysis, we divide all the states in which the receptor can exist ( $k$  in number) into three subsets, as already mentioned in the Discussion. Set A contains the open states ( $k_A$  in number), set B contains the shut states that are occupied while the channel is shut within a burst ( $k_B$  in number), and set C contains long-lived shut states ( $k_C$  in number) such that arrival at a state in set C ends the burst. It is also useful to define the subset of all states that can be occupied during a burst as  $\text{E} = \text{A} \cup \text{B}$  ( $k_E = k_A + k_B$  in number), and the subset of all shut states as  $\text{F} = \text{B} \cup \text{C}$  ( $k_F = k_B + k_C$  in number).

#### Definition of bursts

There is more than one way that a channel activation, or burst, can be defined in terms of mechanism (see Discussion). For the purpose of deriving the time course of a jump to zero concentration, set C must be defined to be an *absorbing* set of shut states, such that when any state in set C is reached, it is impossible to escape from this set at zero concentration. Set B then contains all the other shut states – those from which it is possible to reach at least one of the open states even at zero concentration. These definitions imply that, at zero concentration, the submatrix  $\mathbf{Q}_{\text{CE}} = \mathbf{0}$ . If all the states that are occupied during the burst (set E) are fully liganded then the submatrix  $\mathbf{Q}_{\text{EE}}$ , and hence the time constants for off-relaxation, burst length distribution etc. that are found from it, will not be concentration dependent. More generally, it will be preferable to define channel activations so that they may include, for example, mono-liganded open and shut states. In this case  $\mathbf{Q}_{\text{EE}}$ , and hence burst length probability density functions (pdfs) etc., will be concentration dependent (see Discussion).

#### The burst length distribution

The pdf for the distribution of burst lengths is given (Colquhoun & Hawkes, 1982, 1995*a*) as:

$$f(t) = \boldsymbol{\phi}_b [\exp(\mathbf{Q}_{\text{EE}} t)]_{\text{AA}} (-\mathbf{Q}_{\text{AA}}) \mathbf{e}_b, \quad (\text{A1})$$

where  $\mathbf{e}_b$  is the  $(k_A \times 1)$  ‘end of burst’ vector described there. It thus has  $k_E$  time constants that are the reciprocals of the eigenvalues of  $-\mathbf{Q}_{\text{EE}}$ . In this expression the central term denotes the AA subsection, i.e. the top left  $(k_A \times k_A)$  elements, of  $\exp(\mathbf{Q}_{\text{EE}} t)$ , which is itself a  $(k_E \times k_E)$  matrix.

#### Concentration jump to zero concentration

In general, the time course of any sort of macroscopic current will have time constants that are the reciprocals of the  $k - 1$  non-zero eigenvalues of  $-\mathbf{Q}$  (Colquhoun & Hawkes, 1977). The time course of the current after a step in concentration will be:

$$I(t) = NV \mathbf{p}(0) [\exp(\mathbf{Q}t)] \begin{bmatrix} \boldsymbol{\gamma}_A \\ \mathbf{0} \end{bmatrix}, \quad (\text{A2})$$

where  $\mathbf{p}(0)$  is the  $(1 \times k)$  vector that describes the initial state (see above),  $N$  is the number of channels,  $V$  is the driving force and  $\boldsymbol{\gamma}_A$  is a  $(k_A \times 1)$  vector containing the single-channel conductances of each of the open states (the  $\mathbf{0}$  represents all the shut states). In general, this has  $k - 1$  time constants (the reciprocals of the non-zero eigenvalues of  $\mathbf{Q}$ ). However, when the step is to zero concentration, eqn (A2) reduces (Colquhoun *et al.* 1997) to:

$$I(t) = NV \mathbf{p}_E(0) [\exp(\mathbf{Q}_{\text{EE}} t)]_{\text{EA}} \boldsymbol{\gamma}_A, \quad (\text{A3})$$

where  $\mathbf{p}_E(0)$  is the  $(1 \times k_E)$  vector containing the probability of being in each of the ‘burst’ states at the moment the concentration is stepped to zero (at the end of the concentration pulse in our case). Thus for a step to zero, the number of time constants is only  $k_E$  (the reciprocals of the eigenvalues of  $-\mathbf{Q}_{\text{EE}}$ , as for the burst length pdf), rather



than  $k - 1$ . It should be noted that, in the case of the NMDA receptor, openings *during* the 1 ms application of glutamate are very rare; therefore almost all of the response, rising phase as well as decay, occurs at zero ambient glutamate concentration.

### Time course of current that results from averaging bursts from a steady-state record that have been aligned on their first opening

Since this is a macroscopic current it will, in general, have  $k - 1$  time constants that are the reciprocals of the non-zero eigenvalues of  $-\mathbf{Q}$ . The expression for this current is the same as that given in eqn (A2), except that the initial vector is modified thus:

$$I(t) = NV[\phi_b \mathbf{0}][\exp(\mathbf{Q}t)] \begin{bmatrix} \gamma_A \\ \mathbf{0} \end{bmatrix}, \quad (\text{A4})$$

because  $\phi_b$  gives the state of the system at the moment that a burst starts. This expression asymptotes to the equilibrium current (rather than to zero current), because it represents the average of an ensemble of steady-state records. However, its limiting value, as concentration approaches zero will be given by:

$$I(t) = NV\phi_b[\exp(\mathbf{Q}_{EE}t)]_{AA}\gamma_A. \quad (\text{A5})$$

Thus, once again, we find that there will be  $k_E$  time constants that are the reciprocals of the eigenvalues of  $-\mathbf{Q}_{EE}$ , when the concentration is sufficiently low.

In our experiments the bursts were excised from the steady-state record before averaging (see Methods), so the averaged current asymptotes to zero. In this case the time course for the average is given by eqn (A5) *exactly*, even when the concentration is not zero, as long as  $\phi_b$  and  $\mathbf{Q}_{EE}$  are calculated at the actual concentration used for the steady-state recording. This is because  $\phi_b$  describes the state of the system at the moment the burst starts, and subsequently, if any current is observed, the receptor must still be within the subset, E, of burst states. The time constants are identical with those for the pdf of the burst length (eqn (A1)), but whereas the components of the burst length pdf will all have positive areas, the amplitudes of the components in eqn (A5) may sometimes be negative. If the time constants (the reciprocals of the eigenvalues of  $-\mathbf{Q}_{EE}$ ) are dependent on concentration, they may differ slightly from those found for a jump to zero concentration, but if the steady-state bursts are recorded at a very low concentration, the difference will be small. The initial conditions (e.g.  $p_E(0)$  and  $\phi_b$ ) may be more strongly dependent on concentration, but this will not affect time constants, but only amplitudes.

### Intuitive explanation of the results

It is shown above that it is expected that the following quantities will all have the same time constants (only the relative areas (and hence the overall mean) vary from one to another): (1) the time course of relaxation after a jump to zero concentration; (2) the burst length distribution for bursts recorded at very low concentrations; and (3) the time

course of the average of such bursts, when they are excised and aligned on their first opening. In addition, the same set of  $k_E$  time constants should be found (Colquhoun *et al.* 1997) for: (4) the length of the single channel activation that follows a jump to zero concentration (measured from the start of first opening to the last shutting, so latency is excluded); (5) the length of the activation that follows a jump to zero concentration (from  $t = 0$  to the last shutting, so the latency is included).

At first sight, it appears paradoxical that the time constants should not depend on whether the latency is included or not. The simplest way to look at this is to regard it as a more complex example of the fact that the properties of a simple exponential do not depend on where the timing is started; starting at a later point gives a smaller amplitude but the same time constant. Nevertheless, the example given by Colquhoun & Hawkes (1995a, Fig. 16) certainly suggests that averaged bursts would have a shorter time constant if latency were excluded. Section B of that figure shows an example of what happens if you average records that consist of a long latency followed by a short single opening. The average decays slowly (at a rate that reflects the latency, rather than the length of openings), and aligning the openings would obviously give a much faster decay. The solution to this paradox is that the example cited was simplified to the point where it is misleading. In particular, although correct as it stands, it is not based on a physical mechanism. For any real mechanism, a long latency must arise from the existence of long-lived liganded but shut states, from which opening eventually occurs (directly or indirectly). Thus it must always be possible to return from the open states to these long-lived shut states and then re-open (whether this is common or rare will depend on the particular rates involved, but it is always possible). This means that when the latency is long, the distribution of the lengths of the channel activations that follow the latency must *necessarily* have a long component in it. Thus when the activations are aligned and averaged, the long activations will result in a slow tail in the decay of the average.

- AKAZAWA, C., SHIGEMOTO, R., BESSHO, Y., NAKANISHI, S. & MIZUNO, N. (1994). Differential expression of five *N*-methyl-D-aspartate receptor subunit mRNAs in the cerebellum of developing and adult rats. *Journal of Comparative Neurology* **347**, 150–160.
- BALL, F. G., YEO, G. F., MILNE, R. K., EDESON, R. O., MADSEN, B. W. & SANSOM, M. S. P. (1993). Single ion channel models incorporating aggregation and time interval omission. *Biophysical Journal* **64**, 357–374.
- BÉHÉ, P., STERN, P., WYLLIE, D. J. A., NASSAR, M., SCHOEFFER, R. & COLQUHOUN, D. (1995). Determination of NMDA NR1 subunit copy number in recombinant NMDA receptors. *Proceedings of the Royal Society B* **262**, 205–213.
- CLAPHAM, D. E. & NEHER, E. (1984). Substance P reduces acetylcholine-induced currents in isolated bovine chromaffin cells. *Journal of Physiology* **347**, 255–277.

- CLEMENTS, J. D., LESTER, R. A. J., TONG, G., JAHR, C. E. & WESTBROOK, G. L. (1992). The time course of glutamate in the synaptic cleft. *Science* **238**, 1498–1501.
- COLQUHOUN, D. & HAWKES, A. G. (1977). Relaxation and fluctuations of membrane currents that flow through drug-operated channels. *Proceedings of the Royal Society B* **199**, 231–262.
- COLQUHOUN, D. & HAWKES, A. G. (1982). On the stochastic properties of bursts of single ion channel openings and of clusters of bursts. *Philosophical Transactions of the Royal Society B* **300**, 1–59.
- COLQUHOUN, D. & HAWKES, A. G. (1995a). The principles of the stochastic interpretation of ion channel mechanisms. In *Single-Channel Recording*, ed. SAKMANN, B. & NEHER, E., pp. 397–482. Plenum Press, New York.
- COLQUHOUN, D. & HAWKES, A. G. (1995b). A *Q*-matrix Cookbook. In *Single Channel Recording*, ed. SAKMANN, B. & NEHER, E., pp. 589–633. Plenum Press, New York.
- COLQUHOUN, D., HAWKES, A. G., MERLUSHKIN, A. & EDMONDS, B. (1997). Properties of single ion channel currents elicited by a pulse of agonist concentration or voltage. *Philosophical Transactions of the Royal Society A* **355**, 1–44.
- COLQUHOUN, D. & SAKMANN, B. (1985). Fast events in single-channel currents activated by acetylcholine and its analogues at the frog muscle end-plate. *Journal of Physiology* **369**, 501–557.
- COLQUHOUN, D. & SIGWORTH, F. J. (1995). Fitting and statistical analysis of single-channel records. In *Single-Channel Recording*, ed. SAKMANN, B. & NEHER, E., 2nd edition, pp. 483–587. Plenum Press, New York.
- DZUBAY, J. A. & JAHR, C. E. (1996). Kinetics of NMDA channel opening. *Journal of Neuroscience* **16**, 4129–4134.
- EDMONDS, B. & COLQUHOUN, D. (1992). Rapid decay of averaged single-channel NMDA receptor activations recorded at low agonist concentration. *Proceedings of the Royal Society B*, **250**, 279–286.
- EDMONDS, B., GIBB, A. J. & COLQUHOUN, D. (1995a). Mechanisms of activation of glutamate receptors and the time course of excitatory synaptic currents. *Annual Review of Physiology* **57**, 495–519.
- EDMONDS, B., GIBB, A. J. & COLQUHOUN, D. (1995b). Mechanisms of activation of muscle nicotinic acetylcholine receptors, and the time course of endplate currents. *Annual Review of Physiology* **57**, 469–493.
- GIBB, A. J. & COLQUHOUN, D. (1991). Glutamate activation of a single NMDA receptor-channel produces a cluster of openings. *Proceedings of the Royal Society B* **243**, 39–45.
- GIBB, A. J. & COLQUHOUN, D. (1992). Activation of NMDA receptors by L-glutamate in cells dissociated from adult rat hippocampus. *Journal of Physiology* **456**, 143–179.
- JACKSON, M. B. (1988). Dependence of acetylcholine receptor channel kinetics on agonist concentration in cultured mouse muscle fibres. *Journal of Physiology* **397**, 555–583.
- JACKSON, M. B., WONG, B. S., MORRIS, C. E., LECAR, H. & CHRISTIAN, C. N. (1983). Successive openings of the same acetylcholine receptor channel are correlated in open time. *Biophysical Journal* **42**, 109–114.
- KUNER, T. & SCHOEPFER, R. (1996). Multiple structural elements determine the subunit-specificity of  $Mg^{2+}$  block in NMDA receptor channels. *Journal of Neuroscience* **16**, 3549–3558.
- LESTER, R. A. J., CLEMENTS, J. D., WESTBROOK, G. L. & JAHR, C. E. (1990). Channel kinetics determine the time course of NMDA-receptor mediated synaptic currents. *Nature* **246**, 565–567.
- LESTER, R. A. J. & JAHR, C. E. (1992). NMDA channel behavior depends on agonist affinity. *Journal of Neuroscience* **12**, 635–643.
- LIEBOVITCH, L. S. & TODOROV, A. T. (1996). Using fractals and nonlinear dynamics to determine the physical properties of ion channel proteins. *Critical Reviews in Neurobiology* **10**, 169–187.
- MAGLEBY, K. L. & PALLOTTA, B. S. (1983). Burst kinetics of single calcium-activated potassium channels in cultured rat muscle. *Journal of Physiology* **344**, 605–623.
- MEDINA, I., FILIPPOVA, N., CHARTON, G., ROUGEOLE, S., BEN-ARI, Y., KHRESTCHATISKY, M. & BREGESTOVSKI, P. (1995). Calcium-dependent inactivation of heteromeric NMDA receptor channels expressed in human embryonic kidney cells. *Journal of Physiology* **482**, 567–573.
- MILLER, B. A. & WOOLF, C. J. (1996). Glutamate-mediated slow synaptic currents in neonatal rat deep dorsal horn neurons *in vitro*. *Journal of Neurophysiology* **76**, 1465–1476.
- MOMIYAMA, A., FELDMEYER, D. & CULL-CANDY, S. G. (1996). Identification of a native low-conductance NMDA channel with reduced sensitivity to  $Mg^{2+}$  in rat central neurones. *Journal of Physiology* **494**, 479–492.
- MONYER, H., BURNASHEV, N., LAURIE, D. J., SAKMANN, B. & SEEBURG, P. (1994). Developmental and regional expression in the rat brain and functional properties of four NMDA receptors. *Neuron* **12**, 529–540.
- PAOLETTI, P., ASCHER, P. & NEYTON, J. (1997). High-affinity zinc inhibition of NMDA NR1-NR2A receptors. *Journal of Neuroscience* **17**, 5711–5725.
- STERN, P., BÉHÉ, P., SCHOEPFER, R. & COLQUHOUN, D. (1992). Single-channel conductances of NMDA receptors expressed from cloned cDNAs: comparison with native receptors. *Proceedings of the Royal Society B* **250**, 271–277.
- VICINI, S., WANG, J.-F., LI, J. H., ZHU, W. J., WANG, Y. H., LUO, J. H., WOLFE, B. B. & GRAYSON, D. R. (1998). Functional and pharmacological differences between recombinant *N*-methyl-D-aspartate receptors. *Journal of Neurophysiology* **79**, 555–566.
- WYLLIE, D., BÉHÉ, P., EDMONDS, B. & COLQUHOUN, D. (1997). Fast concentration jumps on recombinant NMDA NR1a/NR2A and NR1a/NR2D channels expressed in *Xenopus* oocytes. *Journal of Physiology* **504.P**, 173P.
- WYLLIE, D. J. A., BÉHÉ, P., NASSAR, M., SCHOEPFER, R. & COLQUHOUN, D. (1996). Single-channel currents from recombinant NMDA NR1a/NR2D receptors expressed in *Xenopus* oocytes. *Proceedings of the Royal Society B* **263**, 1079–1086.
- WYLLIE, D., EDMONDS, B. & COLQUHOUN, D. (1997). Single activations of recombinant NMDA NR1a/NR2A receptors recorded in one-channel patches. *Journal of Physiology* **501.P**, 13P.

#### Acknowledgements

We thank R. Schoepfer and M. Nassar for synthesizing cRNAs, and Professor A. G. Hawkes for statistical advice. D. J. A. W. is a Royal Society University Research Fellow. This work was supported by grants from the MRC and the Royal Society.

#### Corresponding author

D. J. A. Wyllie: Department of Pharmacology, University College London, Gower Street, London WC1E 6BT, UK.

Email: d.wyllie@ucl.ac.uk